Vemurafenib and trametinib reduce expression of CTGF and IL-8 in ^{V600E}BRAF melanoma cells

Mariusz L Hartman, Michal Rozanski, Marta Osrodek, Izabela Zalesna and Malgorzata Czyz

Clinical evidence has revealed that while RAS/RAF/MEK/ERK pathway is a crucial component of melanomagenesis, other signaling pathways can also contribute to the malignant growth and development of resistance to targeted therapies. We explored the response of ^{V600E}BRAF melanoma cells derived from surgical specimens and grown in stem cell medium to vemurafenib and trametinib, drugs targeting the activity of ^{V600E}BRAF and MEK1/2, respectively. Cell growth and apoptosis were monitored by real-time imaging system, immunophenotype and cell cycle by flow cytometry, gene expression by quantitative real-time PCR, immunoblotting and enzyme-linked immunosorbent assay. The ^{V600E}BRAF melanoma cell populations were diverse. Differences in morphology, pigmentation, cell cycle profiles, and immunophenotype were observed. At the molecular level, melanoma cells differed in the phosphorylation of ERK1/2, NF-κB, and β-catenin, and expression of several relevant genes, including *MITF-M*, *DKK1*, *CCND1*, *BRAF*, *CXCL8*, and *CTGF*. Despite having different characteristics, melanoma cells responded similarly to vemurafenib and trametinib. Both drugs reduced ERK1/2 phosphorylation and percentages of cells expressing Ki-67 at high level, inhibited expression of *CCND1* and induced cell cycle arrest in the G_o/G_1 phase. These expected cytostatic effects were accompanied by increased CD271 expression, a marker of stem-like cells. NF-κB activity was reduced by both drugs, however, not completely abolished, whereas the level of active β-catenin was increased by drugs in three out of six cell populations. Interestingly, expression of IL-8 and CTGF was significantly reduced by treatment with vemurafenib and trametinib. Simultaneous inhibition of NF-κB activity and induction of ERK1/2 phosphorylation revealed that CTGF expression depends on ERK1/2 activity but not on NF-κB activity. Both, the positive effects of treatment with vemurafenib and trametinib such as the newly identified CTGF suppression and undesired effects such as increased CD271 expression suggesting selection of melanoma stem-like cells should be considered in the development of combination treatment for melanoma patients.
Laboratory Investigation (2017) **97,** 217–227; doi:10.1038/labinvest.2016.140; published online 9 January 2017

Targeted therapies against elements of the RAF/MEK/ERK pathway have revolutionized the treatment of patients with advanced melanoma prolonging both progression-free and overall survival.[1–3] The response to treatment, however, is not guaranteed, and off-target effects and acquired resistance are observed in the majority of patients.[4–5] The varied clinical efficacy achieved in melanoma patients treated with targeted therapies can be explained by phenotypic heterogeneity, plasticity, multicellular complexity, and reciprocal interactions with the microenvironment that are attributed to metastatic melanoma.[5,6] A better understanding of melanoma response to inhibitors of the BRAF/MEK/ERK pathway is crucial for selecting the most appropriate group of patients for the treatment and developing effective strategies to overcome inherent and acquired resistance.

In the present study, two drugs vemurafenib (PLX4032; Zelboraf), a ^{V600E}BRAF inhibitor, and trametinib (GSK1120212; Mekinist), a MEK1/2 inhibitor, were investigated. Both drugs are approved by the US Food and Drug Administration for the treatment of patients with advanced melanoma harboring mutation in *BRAF* (V600E). Our previous reports indicate that melanoma cells populations derived from surgical specimens and grown in stem cell medium (SCM) better preserve the distinct phenotypic states of melanoma tumors than commercially available cell lines grown as monolayer in serum-containing medium.[7,8] Therefore, likely they represent a more reliable and clinically relevant model system than do xenograft tumors derived from established melanoma cell lines. A most recently published report that examined distinct phenotypic states of melanoma

Department of Molecular Biology of Cancer, Medical University of Lodz, Lodz, Poland
Correspondence: Professor M Czyz, Department of Molecular Biology of Cancer, Medical University of Lodz, 6/8 Mazowiecka Street, Lodz 92-215, Poland.
E-mail: malgorzata.czyz@umed.lodz.pl

tumors by a single-cell RNA sequencing indicates that the same tumor sample can exert transcriptional heterogeneity that is associated with the cell cycle and spatial context.[6] Our study is focused on the whole melanoma cell population cultured *in vitro* as we assume that the interactions between different subpopulations might influence melanoma phenotype and response to drug treatment.[8–10]

Six melanoma cell populations with activating mutation in *BRAF* (V600E) were used to explore the melanoma response to vemurafenib and trametinib. Cells were extensively investigated to show similarities and differences at the molecular and cellular levels. Having well characterized cell populations and their targeted response to vemurafenib and trametinib, we have focused on drug-induced alterations in cell composition, particularly CD271^{high} stem-like cells [11–13] *vs* Ki-67^{high} proliferating cells. In addition, the influence of the drugs on key components of other than RAF/MEK/ERK signaling pathway, namely NF-κB and β-catenin signaling, was investigated at the molecular level. MITF-M, a transcription factor crucial for melanocyte differentiation and melanoma maintenance,[14–16] DKK1, an inhibitor of the WNT/β-catenin pathway,[17] whose expression is strongly reduced in melanoma cells compared with melanocytes,[7,18] CTGF (CCN2) recently considered as a therapeutic target for metastatic melanoma[19] and interleukin 8 (IL-8, encoded by *CXCL8*), which exhibits significant overexpression in melanoma[20] were investigated among others.

MATERIALS AND METHODS
Drugs
Parthenolide was purchased from Biomol (Exeter, UK), vemurafenib and trametinib from Selleck Chemicals LLC (Houston, TX, USA).

Tumor Tissues and Cell Culture
Melanoma cell populations from drug-naive patients were investigated. The study was approved by Ethical Commission of Medical University of Lodz. Informed consent was obtained from all patients. Tumor tissues were processed immediately after surgical procurement and suspensions of melanoma cells for culturing were generated within 2 h. Cells harboring mutation [V600E]BRAF that were successfully propagated were named DMBC11, DMBC12, DMBC21, DMBC28, DMBC29, and DMBC33 (Department of Molecular Biology of Cancer, DMBC). Melanoma cells were maintained in SCM as described previously.[21]

For experiments, melanoma cells were left to grow overnight before being treated with 10 µM vemurafenib or 50 nM trametinib. Then, cells were collected for RNA isolation (after 24 h), protein lysates (after 44 h), cell cycle and immunophenotype analysis (after 44 h). Culture medium was frozen for the IL-8 secretion analysis. Transfection of melanoma cells with specific CTGF siRNA or control siRNA (Santa Cruz Biotechnology, Santa Cruz, CA, USA) was performed by using AMAXA NHEM-Neo Nucleofector Kit and Nucleofector 2b

device (Lonza, Basel, Switzerland) according to the manufacturer's protocol. Melanoma cells were collected for cell lysate preparation 24 h after transfection. Human full-length CTGF recombinant protein, purchased from PeproTech Inc (Rocky Hill, NJ, USA), was used at 250 ng/ml for 24 h. Parthenolide and trametinib were used alone or in combination at indicated concentrations, and RNA was isolated after 6 h and cell lysates were prepared after 4 h of incubation.

Microscopy
Changes in cell morphology were registered with a digital Olympus camera (C-5050) attached to Olympus microscope (CKX41, Olympus, London, UK).

A Time-Lapse Fluorescence Microscopy
For cell proliferation, apoptosis and CFSE analysis, a time-lapse fluorescence microscope system (IncuCyte, Essen Bioscience) was used. The data were analyzed using IncuCyte Zoom original software. Proliferation was assessed as changes in the area occupied by melanoma cells in control, vehicle-treated (0.1% DMSO) and drug-treated cultures (% of confluence) over time. For apoptosis assay, melanoma cells were seeded in 96-well plates at 8×10^3 cells/well with IncuCyte Caspase-3/7 Apoptosis Assay Reagent at 4 µM and exposed to 10 µM vemurafenib, 50 nM trametinib or vehicle for 3 days. Activation of caspase-3/7 was monitored every 3 h using live-cell imaging and quantified using the IncuCyte ZOOM basic analyzer. It was expressed as the percentage of confluence of apoptotic cells divided by the percentage of confluence of all cells. For CFSE analysis, melanoma cells were stained with 1.5 µM CFSE (carboxyfluorescein diacetate succinimidyl ester) for 30 min at 37 °C, washed twice, seeded in 12-well plates at 1.25×10^5 cells/well and exposed to 10 µM vemurafenib, 50 nM trametinib or vehicle for 5 days. Changes in green fluorescence emission were monitored every 6 h. Percentages of label retaining cells were calculated in the same way as percentages of apoptotic cells, however, the thresholds were set at very low levels to filter out non-fluorescent cells.

Acid Phosphatase Activity Assay
Doubling time was calculated based on the colorimetric measurement of acid phosphatase activity.[21] Briefly, melanoma cells (4×10^3) were grown for 24 h and 48 h, then the plates were centrifuged and medium was replaced with assay buffer containing 0.1 mmol/dm³ of sodium acetate pH = 5, 0.1% Triton X-100 and 5 mmol/dm³ *p*-nitrophenyl phosphate (Calbiochem, Darmstadt, Germany). After 2 h of incubation, the reaction was inhibited by 1 mmol/dm³ NaOH, and the absorbance was measured at 405 nm using microplate reader Infinite M200Pro (Tecan, Salzburg, Austria). The doubling time was calculated using the formula $DT = (t - t_0)\log2 / (\log A - \log A_0)$, in which t and t_0 are the time points at which the cells were collected and A and A_0 are the absorbance values at times t and t_0, respectively.

Flow Cytometry

Melanoma cells were left to grow overnight before being treated with drugs for 44 h. After treatment, 70% of cells were immunophenotyped and 30% were used for cell cycle analysis. In immunophenotype analysis, isotype controls were included in each experiment. To exclude dead cells from the analysis, LIVE/DEAD Fixable Violet Dead Cell Stain Kit (Life Technologies, Eugene, OR, USA) was used. Antibodies against CD271 (PE-conjugated) and Ki-67 (Alexa Fluor 647-conjugated) were from BD Pharmingen (San Jose, CA, USA). For intracellular staining, cells were fixed with 4% paraformaldehyde and permeabilized with 0.1% Triton X-100 in PBS for 20 min. Flow cytometric data were acquired with FACSVerse (BD Biosciences, San Jose, CA, USA), and analyzed using BD FACSuite. For cell cycle analysis, PI/RNase Staining Buffer (BD Pharmingen) was used. ModFit LT 3.0 software was used to calculate the percentages of cells in each cell cycle phase.

RNA Isolation, cDNA Synthesis, and Quantitative RT-PCR (qRT-PCR)

Total RNA was isolated and purified using Total RNA Isolation kit with mini column system (A&A Biotechnology, Gdynia, Poland). Total RNA (1 µg) was transcribed into cDNA using 300 ng of random primers and SuperScript II Reverse Transcriptase (Invitrogen Life Technologies, Carlsbad, CA, USA). The evaluation of mRNA expression of selected genes was performed by quantitative real-time polymerase chain reaction using the Rotor-Gene 3000 Real-Time DNA analysis system (Corbett Research, Morklake, Australia). Amplification was performed using KAPA SYBR FAST qPCR Kit Universal 2X qPCR Master Mix (Kapa Biosystems, Cape Town, South Africa), 200 nM of each primer and 25 ng cDNA template per reaction. Primer sequence for *BRAF* was: 5′-TCTTTCCCCAAATTCTCGCCT-3′ (forward) and 5′-TCAGTGGACAGGAAACGCAC-3′ (reverse). Sequences of other primers used in qRT-PCR were shown elsewhere.[7,22–24] To calculate the relative expression of target genes *vs* a reference gene *RPS17,* a mathematical model including an efficiency correction was used.

Western Blots

Melanoma cells were lysed in RIPA buffer containing 50 mmol/l Tris-HCl pH 8.0, 150 mmol/l NaCl, 1% Triton X-100, 0.5% sodium deoxycholate, 0.1% SDS supplemented with freshly added protease and phosphatase inhibitors (Sigma-Aldrich). Cell lysates were diluted in 2× Laemmli buffer and protein samples (15 µg each) were loaded on 7% SDS-polyacrylamide gel. The proteins were transferred onto an Immobilon-P PVDF membrane (Millipore, Billerica, MA, USA). The membrane was incubated in a blocking solution: 5% nonfat milk in PBS-Tween 0.05% or 5% phospho-BLOCKER (Cell Biolabs, San Diego, CA, USA) in PBS-Tween 0.05%. Primary antibodies detecting PARP and total β-catenin were from Santa Cruz Biotechnology, active β-catenin (dephosphorylated on Ser[37] and Thr[41]) from

Millipore (Temecula, CA, USA), MITF, p-p65 (Ser[536]), p65, p-ERK1/2 (Thr[202]/Tyr[204]), ERK1/2 from Cell Signaling Technology (Danvers, MA, USA), [V600E]BRAF from Biomol (Malvern, PA, USA). Immunodetection of β-actin (Sigma-Aldrich) was used as a loading control.

Enzyme-Linked Immunosorbent Assay (ELISA)

ELISA kit Quantikine High Sensitivity Human CXCL8/IL-8 (R&D Systems, Minneapolis, MN, USA) was used to determine IL-8 secretion to the culture medium by melanoma cells, and was performed according to the manufacturer's instructions. The optical density of each well was determined using a microplate reader Infinite M200Pro (Tecan). Concentrations of IL-8 in the medium samples were obtained by using a four parameter logistic (4-PL) curve fit.

Statistical Analysis

Data show the mean of at least three independent experiments ± s.d. unless stated otherwise. Statistically significant results were considered at $*P < 0.05$.

RESULTS

The Phenotype of Melanoma Cell Populations Derived from Surgical Specimens and Grown in SCM is Diverse

Six melanoma cell populations derived from surgical specimens and designated DMBC11, DMBC12, DMBC21, DMBC28, DMBC29, and DMBC33 were used in this study. All of them harbor mutation in *BRAF* resulting in a high level of active [V600E]BRAF kinase as shown for DMBC28, DMBC29, and DMBC33 cells (Figure 1a) or published previously for other cell lines.[10] They showed different morphology (Figure 1a) when grown in SCM. DMBC11, DMBC12, and DMBC33 remained floating as single cells or cell aggregates. DMBC21, DMBC28, and DMBC29 represented 'semi-adherent' cultures, in which both floating and adherent cells were observed. MITF-M was expressed in DMBC21, DMBC28, DMBC29 and DMBC33 cells at a very high level (Figures 1a and d); however, only one cell population DMBC33 was highly pigmented (Figure 1a). Cell cycle analysis revealed that DMBC11, DMBC12, and DMBC28 cell populations were fast-cycling, whereas in other cell lines more cells were accumulated in G_0/G_1 phase with the highest percentage of G_0/G_1 phase-arrested cells in DMBC33 population (Figure 1b). Accordingly, the highest doubling time, 107.7 h, was observed in DMBC33 population, the lowest, 17.6 h and 18.8 h in DMBC11 and DMBC12, respectively.

Analysis of cell functionality indicated that DMBC12 and DMBC33 cell lines had elevated levels of phosphorylated ERK1/2 in comparison with other cell lines (Figure 1c). DMBC33 cells exerted a high level of active β-catenin and the highest activity of NF-κB assessed as phosphorylation of p65 (Figure 1c), but other cell populations also showed constitutive activity of this transcription factor. A few genes were then chosen to assess their transcript levels (Figure 1d). *CCND1*, *CXCL8*, and *BRAF* were expressed at much higher
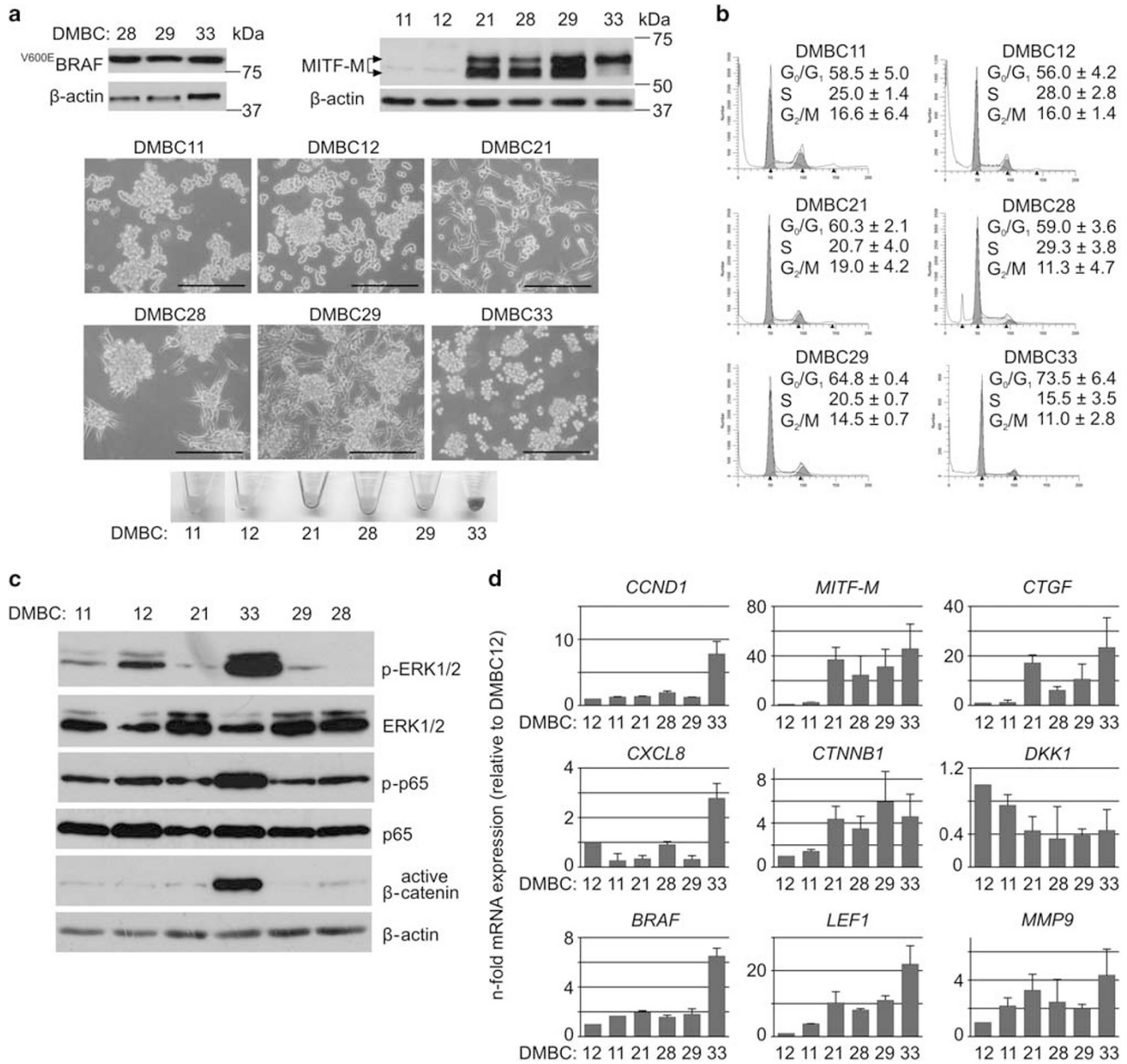
Figure 1 Cellular and molecular characteristics of melanoma cell populations derived from surgical specimens and cultured in SCM. (**a**) All cell populations were [V600E]BRAF-positive as shown for DMBC28, DMBC29, and DMBC33 and published elsewhere.[10] Cell cultures showed different morphology (scale bar, 250 μm). Four out of the six cell populations were MITF-M[high] but only one was strongly pigmented. (**b**) Cell cycle profiles were determined by flow cytometry. Representative histograms and their quantification from two independent experiments are shown. ModFit LT 3.0 software was used to calculate the percentages of viable cells in cell cycle phases. (**c**) Representative western blot images showing basal activity of several pathways, including RAS/RAF/MEK/ERK, NF-κB and WNT/β-catenin pathway in melanoma cells. β-actin was used as a loading control. (**d**) Basal expression levels of several genes recognized as important for melanoma development were determined by qRT-PCR and normalized to the expression of a reference gene *RPS17*. Gene expression levels in each melanoma cell population were expressed relatively to the median of all six populations. Bars represent the mean values ± s.d. DMBC, melanoma cell populations obtained in Department of Molecular Biology of Cancer from surgical specimens.

levels in the DMBC33 cell lines than in other cell lines, which together with the highest ERK1/2 activity might reflect the hyperactivity of the RAS/RAF/MEK/ERK pathway in this cell line. The MITF-M^{high} cells, DMBC21, DMBC28, DMBC29, and DMBC33 expressed *CTNNB1, LEF1*, and *CTGF* at higher levels than MITF-M^{low} cells, whereas *DKK1*, the inhibitor of

the WNT/β-catenin pathway, was expressed at a high level in MITF-M^{low} cells, DMBC11 and DMBC12. Thus, the investigated melanoma cell lines while all harboring [V600E]BRAF, show diverse phenotypes as the result of various activity of the major signaling pathways (summarized in Table 1). Lack of consistency between different features

Table 1 Cellular and molecular characteristics of melanoma cell populations derived from surgical specimens and grown in SCM.

	Estimated at the level of	DMBC11	DMBC12	DMBC21	DMBC28	DMBC29	DMBC33
^{V600E}BRAF	Protein	+	+	+	+	+	+
Distribution in cell cycle	Cell population	High S	High S		High S		High G_0/G_1
Pigmentation	Cell population	−	−	−	−	−	+
Doubling time	Cell population	Low	Low	Medium	Medium	Medium	High
ERK1/2 activity	Protein phosphorylation	Medium	High	Low	Low	Low	Very high
NF-kB activity	Protein (p65) phosphorylation	Medium	Medium	Medium	Medium	Medium	High
MITF-M	Protein	Low	Low	High	High	High	Medium
CTGF	Transcript	Low	Low	High	High	High	High
LEF1	Transcript	Low	Low	High	High	High	High
β-catenin	Transcript	Low	Low	High	High	High	High
DKK1	Transcript	High	High	Low	Low	Low	Low
Active β-catenin	Protein phosphorylation	Low	Low	Low	Low	Low	High
Cyclin D1	Transcript	Low	Low	Low	Low	Low	High
IL-8	Transcript	Low	Medium	Low	Medium	Low	High
IL-8	Secretion	Low	Medium	Medium	Medium	Medium	High
Ki-67^{high} cells	Cell population	High	High	Medium	High	Medium	Low
CD271^{high} cells	Cell population	Medium	Low	Low	Medium	Low	Medium

suggests that each cell population contained a broad spectrum of subpopulations with different, strongly pronounced phenotypes, which collectively defined the behavior of the whole population. For instance, DMBC33 cell population having highly active ERK1/2 and NF-κB pathways at the same time exerted the highest doubling time, high percentage of cells in G_0/G_1 phase of cell cycle and low percentage of cells expressing Ki-67 at high level (Supplementary Figure 1a). This can be explained only as inherent phenotypic heterogeneity of DMBC33 population. DMBC12 cell population was less phenotypically heterogeneous as for example high activity of ERK1/2 was accompanied by a high cell cycling rate and percentage of cells expressing Ki-67 at high level (Supplementary Figure 1a).

Cytostatic Effects of Vemurafenib and Trametinib Driven by Inhibition of the BRAF/MEK/ERK Pathway were Validated at the Cellular and Molecular Level

First, all cell populations were investigated whether they responded to vemurafenib and trametinib. Concentrations of drugs, 10 μM for vemurafenib and 50 nM for trametinib, were then chosen based on their similar cytostatic effects observed in live-cell time-lapse imaging system IncuCyte (Figure 2a). The targeted activity of vemurafenib and trametinib was validated by Western blotting. The ERK1/2 activity was abolished after 4 h of treatment (not shown) and was still inhibited after 2 additional days of incubation with either drug (Figure 2b). This was accompanied by cell cycle arrest in

G_0/G_1 phase (Figure 2c). The level of cyclin D1 transcript was also significantly diminished in all cell populations, especially in DMBC33 (Figure 2d), which exerted the highest basal level of *CCND1* expression (Figure 1e). We also observed a strong influence of vemurafenib and trametinib on the fraction of cells expressing Ki-67 at high level across all investigated melanoma cell populations (Figure 3b). When apoptosis was assessed by measuring changes in the percentages of cells with high activity of caspase 3/7, only DMBC33 cells did not develop apoptotic cell death response to drug treatment during 72 h of incubation (Figure 2e). PARP cleavage confirmed these results (Figure 2f).

Cytostatic Effects of Vemurafenib and Trametinib are Accompanied by Increased Percentages of Slow-Dividing Cells and Elevated Expression of CD271

Next, to investigate a drug influence on slow-dividing cells time-lapse microscopy was used to measure the retention of CFSE in real time. CFSE is a prodrug for an intracellular green-fluorescent dye that is partitioned evenly between daughter cells upon cell division without causing reduction of cell viability. Over the course of 5 days, untreated cells or cells treated with vehicle diluted out CFSE and decreased in fluorescence intensity more efficiently than vemurafenib- or trametinib-treated cells. DMBC33 cell population was the most efficient in retaining a fluorescence label, which was further enhanced by drug treatment (Figure 3a). All these results might be explained as cytostatic effects of vemurafenib
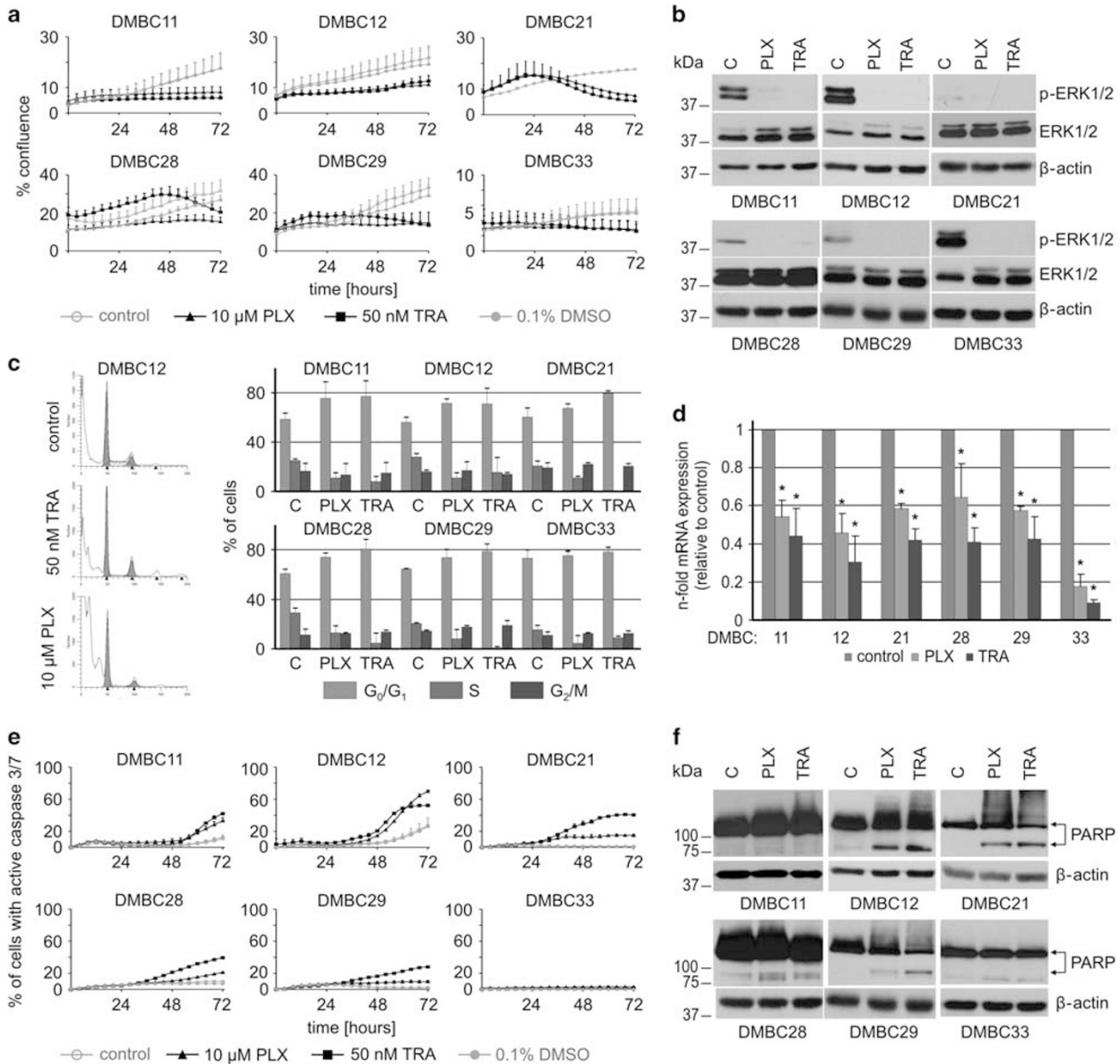
Figure 2 All melanoma cell populations respond to vemurafenib (PLX) and trametinib (TRA) treatment. (**a**). Proliferation time-courses. Cell proliferation was monitored by analyzing the occupied area (% confluence) of cell images over time using IncuCyte. Cytostatic effects of drugs were observed in all tested populations, and reached similar levels for vemurafenib at 10 μM and trametinib at 50 nM. (**b**). Representative western blot images showing changes in the level of phosphorylated ERK1/2 after 44 h of incubation with either 10 μM PLX or 50 nM TRA. β-actin was used as a loading control. (**c**). PLX and TRA accumulated melanoma cells in G_0/G_1 phase. Distribution of melanoma cells in cell cycle phases was determined by flow cytometry. Representative histograms for DMBC12 cell population and the quantification for all melanoma cell lines are shown. ModFit LT 3.0 software was used to calculate the percentages of viable cells in cell cycle phases. Bars represent the mean values ± s.d. $n = 2$. (**d**). *CCND1* mRNA fold change after 24 h of incubation with 10 μM PLX and 50 nM TRA. The expression level of *CCND1* was normalized to the expression of a reference gene *RPS17*. Data are presented as fold change in drug-treated samples *vs* control. Differences are considered significant at *$P < 0.05$. (**e** and **f**). Apoptosis induced by PLX and TRA in melanoma cells. (**e**). Percent of apoptotic cells with high caspase 3/7 activity was assessed in time-lapse imaging system IncuCyte over the course of 72 h. (**f**). Apoptosis shown as PARP cleavage after 44 h of incubation with drugs. Equal loading was confirmed by β-actin. C, control.

and trametinib or as drug-induced selection of slow-dividing cells. As reduced percentages of cells expressing Ki-67 at high level (Figure 3b and Supplementary Figure 1a) were accompanied with increased expression of CD271 and mutually exclusive expression of CD271 and Ki-67 (CD271^{high}/Ki67^{low}) (Figure 3c), all this suggests that the fraction of more primitive, slow-cycling cells remained less affected by the drug treatment.
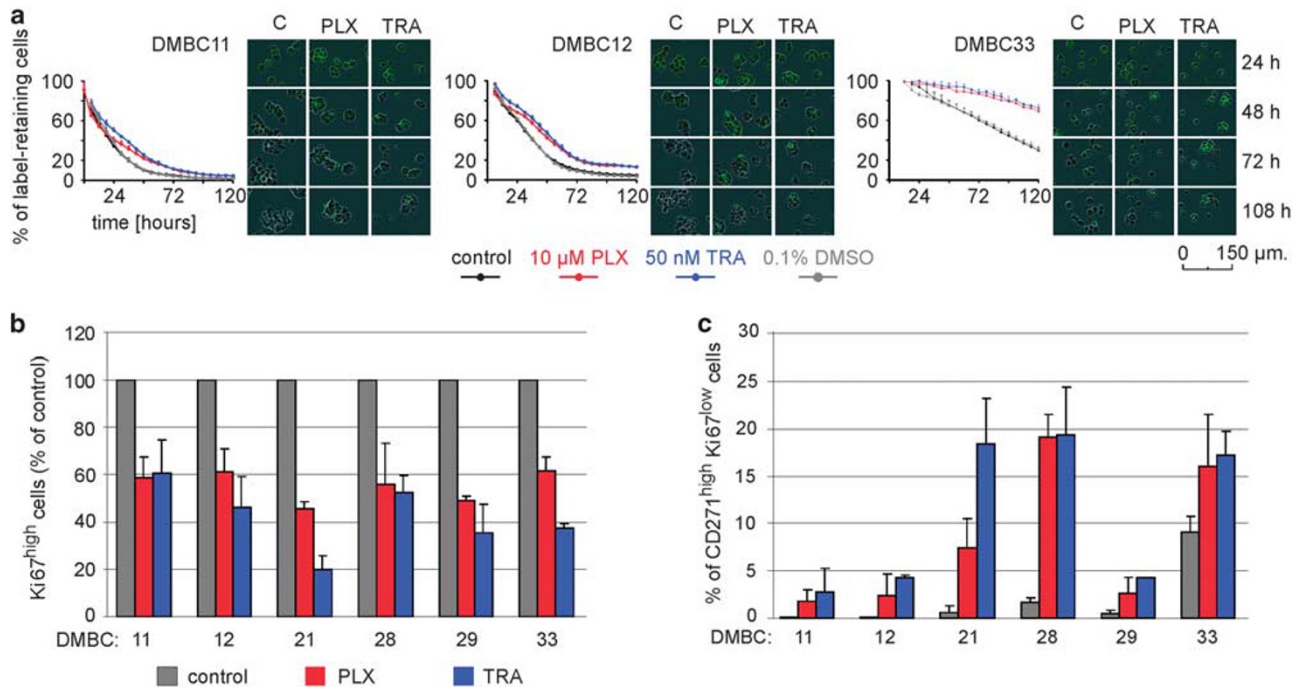
Figure 3 Vemurafenib (PLX) and trametinib (TRA) significantly reduce the percentage of Ki-67^{high} cells and increase the subpopulation of CD271^{high}/Ki-67^{low} cells. (**a**) Limited activity of targeted drugs against a subpopulation of slow-cycling label-retaining melanoma cells. Melanoma cells were stained with CFSE and treated with vehicle (DMSO), PLX or TRA, and the remaining CFSE fluorescence was assessed by timelapse imaging system IncuCyte. Representative microphotographs taken at the indicated time points are included. (**b**) Drug-induced changes in the fraction of Ki-67^{high} cells are expressed as percent of control. (**c**) The fraction of CD271^{high}/Ki-67^{low} cells is presented as % of all viable cells in the control and drug-treated cultures. All changes were statistically significant ($P < 0.05$).

NF-κB and β-Catenin Activities are Only Slightly Affected by Vemurafenib and Trametinib but IL-8 and CTGF Expression is Significantly Reduced by these Drugs

Next, the influence of vemurafenib and trametinib on other pathways than RAF/MEK/ERK signaling was investigated (Figure 4a). The activity of the WNT/β-catenin pathway, which was assessed as the level of active, dephosphorylated β-catenin, was elevated especially in DMBC12 and DMBC21 cells but it remained unchanged in DMBC33 cell population (Figure 4a), in which the WNT/β-catenin pathway was already highly active (Figure 1c). The activity of NF-κB was reduced by both drugs, however, not completely abolished (Figure 4a). The expression of an NF-κB-dependent gene, *CXCL8* was significantly reduced by vemurafenib and trametinib (Figure 4b), and the secretion of IL-8 into the culture medium was also lowered (Figure 4c). The strongest reduction of the IL-8 production was observed in DMBC33 cell culture, in which the average secretion of IL-8 was also the highest in untreated culture (1272 pg IL-8/10[5] cells). Besides *CXCL8*, whose expression was most strongly affected, also expression of *CTGF* was significantly ($P < 0.05$) down-regulated by vemurafenib and trametinib in all investigated melanoma cell populations (Figure 4b). [V600E]BRAF/MEK inhibition did not substantially change expression of *MITF-M*, *CTNNB1*, *DKK1*, *MMP9*, *LEF1*, and *BRAF* at transcript levels as assessed by qRT-PCR (Supplementary Figure 1b).

CTGF Expression Depends on ERK1/2 Activity

As CTGF transcript level was reduced by vemurafenib and trametinib, we hypothesized that *CTGF* expression might be ERK1/2-dependent. It could be also NF-κB-dependent as the activity of this transcription factor was also diminished by both drugs. To distinguish between these two possibilities, parthenolide was used. As recently shown by our laboratory this compound, known mainly as an NF-κB inhibitor, efficiently increases ERK1/2 activity.[10] Thus, by using parthenolide it was possible to block NF-κB activity and increase ERK1/2 activity at the same time. And indeed immunoblots revealed a dramatic increase in the level of phosphorylated ERK1/2 already after 4 h of incubation, whereas the level of phosphorylated p65 was substantially reduced (Figure 5a). These effects were accompanied by a significant increase in CTGF transcript level as shown for DMBC21, DMBC29 and DMBC33 cells (Figure 5b) indicating that CTGF expression might depend on ERK1/2 activity but not on NF-κB activity. *CTGF* expression was even more enhanced in DMBC11 and DMBC12 reaching a 7.6-fold ± 4.0 and 21.2-fold ± 3.3 increase in comparison to untreated cells, respectively (Supplementary Figure 2a), but of note the basal level of CTGF transcript was very low in those cells (Figure 1d). When parthenolide was combined with trametinib, the CTGF transcript level was not significantly changed when compared with its level in untreated cells. As *CTGF* expression was
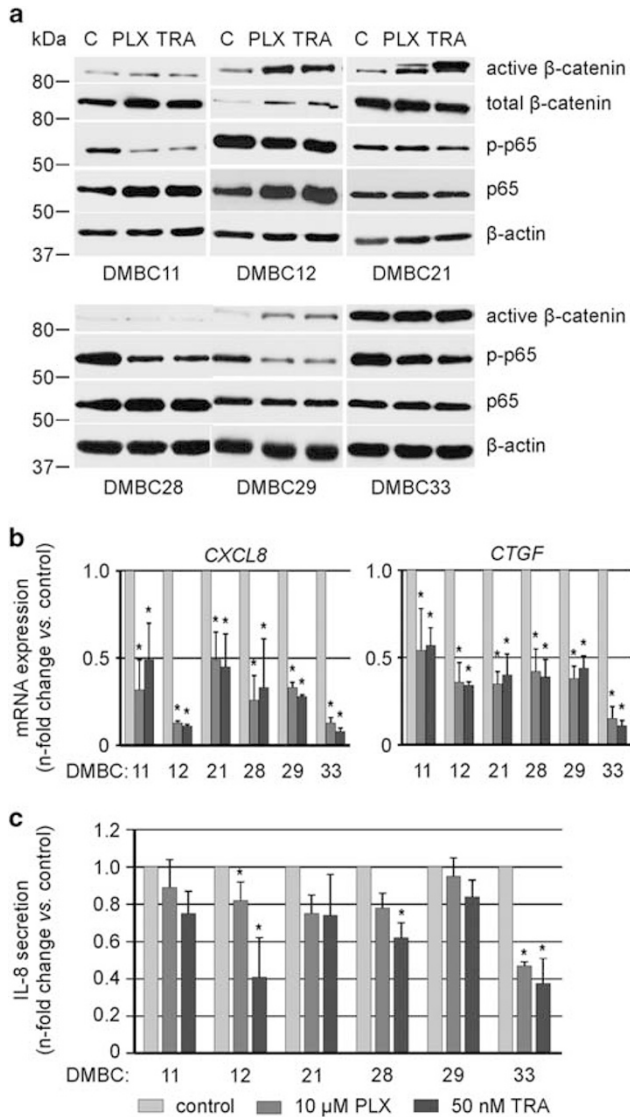
Figure 4 Effects of vemurafenib (PLX) and trametinib (TRA) in phenotypically diverse melanoma cell populations. (**a**) Cells were treated with 10 μM PLX and 50 nM TRA for 44 h and the levels of active β-catenin, total β-catenin, phosphorylated p65 (p-p65), and p65 were assessed by immunoblotting. Equal loading was confirmed by β-actin. Representative results are shown. (**b**) qRT-PCR validation of changes in the expression of *CXCL8* and *CTGF* in melanoma cells after 24 h of incubation with 10 μM PLX and 50 nM TRA relative to the respective control. The expression is normalized to the expression of a reference gene *RPS17*. Data are presented as a fold change in drug-treated samples *vs* control. Differences are considered significant at *$P < 0.05$. (**c**) IL-8 secretion assessed by ELISA in culture medium collected after 24 h incubation with indicated drug or vehicle. Data are presented as fold change in drug-treated cultures *vs* control culture, in which the secretion level of IL-8 was set as 1. The mean values and s.d. were calculated from at least two experiments. Differences were considered significant at *$P < 0.05$.

reduced by drugs inhibiting the RAF/MEK/ERK pathway (trametinib and vemurafenib) and increased by ERK1/2 inducer (parthenolide), it might indicate that *CTGF* expression depends on ERK1/2 activity. As the activity of AP-1 was

found to be ERK pathway-dependent and might influence the expression of *CTGF*, we assessed the level of phosphorylated c-JUN, a subunit of AP-1. Levels of active c-JUN (phosphorylated c-JUN, p-c-JUN) remained unchanged in melanoma cells after treatment with vemurafenib and trametinib (Supplementary Figure 2b), indicating that AP-1 did not contribute to ERK1/2-induced upregulation of CTGF expression. Next, we performed mRNA decay assay. We demonstrated that CTGF transcript stability was not substantially altered in the presence of vemurafenib or trametinib (Supplementary Figure 2c). We also determined the consequences of changing the level of CTGF on ERK1/2 activity. In the first approach, *CTGF* expression was blocked with siRNA. A direct blockade of *CTGF* expression did not result in substantial changes of ERK1/2 phosphorylation as shown for CTGF[high] p-ERK1/2^{low} DMBC21 cells and CTGF[high] p-ERK1/2^{high} DMBC33 cells (Figure 5c). As a second approach, we checked whether exogenous CTGF can change the phosphorylation of ERK1/2 and p65 subunit of NF-κB. Exogenous CTGF neither induced ERK1/2 activity nor prevented its inhibition by vemurafenib and trametinib as shown for p-ERK1/2^{high} DMBC33 cells (Figure 5d). No induction of ERK1/2 phosphorylation was also observed in p-ERK1/2[low] DMBC21 and DMBC29 cells (Figure 5d). The exogenous CTGF also did not substantially change the phosphorylation of p65 (Figure 5d). Therefore, it is reasonable to conclude that CTGF does not markedly influence the RAF/MEK/ERK and NF-κB signaling pathways.

DISCUSSION

The inhibitors of [V600E]BRAF and MEK1/2 have brought major improvements in blocking constitutively active RAF/MEK/ERK pathway that is critical for melanoma development. As the RAF/MEK/ERK pathway is strongly connected with other signaling pathways, both its hyperactivation observed in cancer and its inhibition by targeted treatment can induce a plethora of consequences at the molecular and cellular levels.[25] The major and desired effect of using vemurafenib and trametinib in melanoma treatment is the inhibition of cell proliferation and tumor growth. Other consequences of RAF/MEK/ERK inhibition remain largely elusive. Their investigation might bring new directions of studies to overcome intrinsic, adaptive, and acquired resistance.

The complex effects of [V600E]BRAF and MEK1/2 inhibition presented in this study comprise both positive and negative effects. As previously demonstrated in numerous *in vitro* and *in vivo* studies [reviewed in Marzuka *et al*[26]] vemurafenib and trametinib strongly inhibited ERK1/2 activity followed by induction of cell cycle arrest in G_0/G_1 phase. As the consequence of ERK1/2 inhibition, the expression of cyclin D1 was significantly diminished, regardless of its basal level. Apoptosis, which is suppressed by aberrant ERK1/2 activity but is not the major outcome of targeted therapy,[27,28] was not highly pronounced also in the present study, especially in DMBC33 cell population. It has been demonstrated that
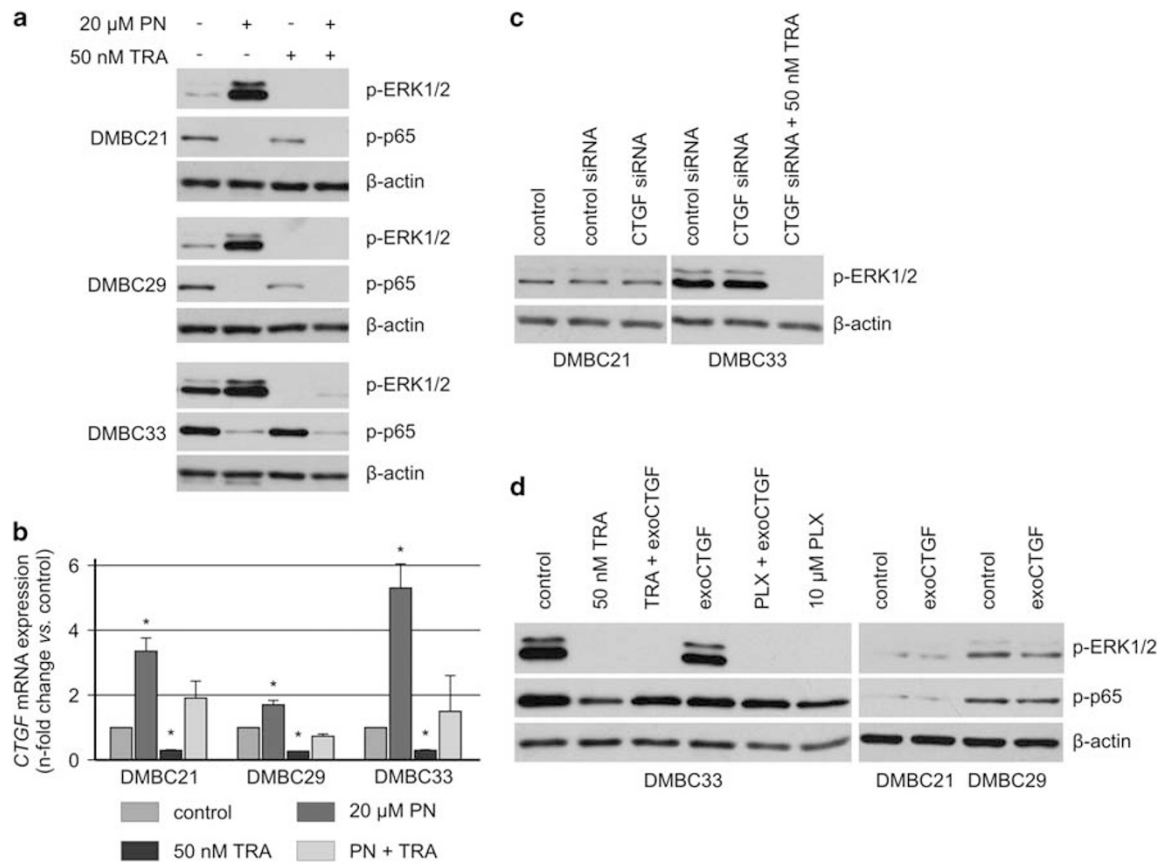
Figure 5 Expression of *CTGF* depends on ERK1/2 activity but not on NF-κB activity. (**a**) Parthenolide (PN) was used as a tool that is capable to reduce NF-κB activity and increase ERK1/2 phosphorylation[15] as shown in three different melanoma cell populations, DMBC21, DMBC29, and DMBC33. (**b**) Expression of *CTGF* was increased in the presence of PN as assessed by qRT-PCR. Differences were considered significant at *$P<0.05$. (**c**). ERK1/2 activation in melanoma cells transfected with control siRNA and CTGF siRNA was determined by immunoblotting. (**d**) The levels of phosphorylated ERK1/2 in control cells and cells treated with exogenous CTGF (250 ng/ml) used alone or in combination with either vemurafenib or trametinib were determined by immunoblotting. β-actin was used as a loading control.

induction of apoptosis can be inhibited by pretreatment of melanoma cells with LiCl, a β-catenin stabilizing agent, and β-catenin can attenuate vemurafenib efficacy and mediate acquired resistance.[29] Our results showing an elevated level of active β-catenin in cell population not responding with apoptosis to vemurafenib and trametinib suggest that β-catenin can positively influence cell survival also in treatment-naive [V600E]BRAF melanomas. This is in agreement with reports suggesting that active β-catenin signaling is associated with more aggressive melanoma and worse survival of patients.[30,31] This also indicates that inhibition of WNT/β-catenin signaling[17] should be considered as a part of therapy in a group of melanoma patients with elevated level of active β-catenin. We have recently demonstrated that pentoxifylline, a drug approved by the US Food and Drug Administration in the treatment of peripheral arterial disease, inhibits the activity of the canonical WNT pathway in melanoma cell populations with high basal activity of this signaling.[24]

The higher percentage of slow-cycling melanoma cells retaining CFSE in the drug-treated cell populations in comparison to the control cell populations might indicate

that vemurafenib and trametinib just exerted cytostatic effects. However, when these results are combined with results showing elevated expression of CD271, drug effects might be interpreted as a selection of slowly dividing melanoma stem-like cells. High level of CD271 was assessed in vemurafenib-resistant brain and lung metastasizing melanoma cells.[32] Selection of CD271-positive cells by vemurafenib in melanoma cell lines was shown to be NF-κB-dependent.[33] In another study, however, NF-κB pathway was inactive in CD271-positive melanoma cells, and was activated when this marker was lost.[34] In the present study, vemurafenib and trametinib while increasing the percentage of CD271^{high} cells diminished activity of NF-κB shown as reduced phosphorylation of p65 subunit and IL-8 expression. Therefore, the role of the NF-κB pathway in the regulation of CD271 needs further examination. Nevertheless, our results support the notion that slow-cycling CD271^{high} cells are selected by vemurafenib and trametinib, which might be a base for acquired resistance. It was recently demonstrated that CD271 (NGFR) is connected with AXL-high program, and a subset of drug-resistant melanoma biopsies exhibited

increased activity of this program when compared with biopsies taken before treatment.[6]

CXCL8 expression was the most significantly downregulated gene by vemurafenib and trametinib among investigated genes. IL-8 and its receptors are important for melanoma progression and metastasis.[20] *CXCL8* expression is NF-κB-dependent, which is consistent with a concomitant inhibition of NF-κB activity and *CXCL8* expression observed in this study. It was demonstrated in biopsies collected from patient with metastatic melanoma that treatment with either vemurafenib alone or dabrafenib in combination with trametinib was associated with reduced levels of IL-8 and IL-6.[35] Wilson *et al.* have shown that IL-8 is produced predominantly by ABCB5 (ATP-binding cassette, subfamily B, member 5)-negative melanoma cells comprising the bulk population.[36] Our results showing that vemurafenib and trametinib while reducing IL-8 expression increased the frequency of CD271^{high}/Ki-67^{low} cells, are in line with this notion, especially if we consider that both stem cell markers, ABCB5 and CD271 were found to be co-expressed in clinical melanoma specimens.[37] In the present study, besides IL-8 also CTGF was strongly downregulated by vemurafenib and trametinib. Lin *et al.* have shown that CTGF regulates *CXCL8* promoter via NF-κB signaling.[38] As *CTGF* and *CXCL8* were concomitantly downregulated by vemurafenib and trametinib, we assumed that CTGF might contribute to increased *CXCL8* expression also in melanoma. However, our results revealed that CTGF neither influenced *CXCL8* expression nor NF-κB activity in melanoma cells.

CTGF (CCN2) has multiple roles as oncogene and tumor suppressor in diverse cancer types.[39–44] It is secreted and functions as a ligand of integrins, mainly αvβ3, to regulate cell proliferation, apoptosis, cell migration, angiogenesis, and anoikis.[45] Recent findings have suggested various functional implications of CTGF in melanoma development.[19,46–48] The expression of CTGF is upregulated in advanced stages of melanoma[49] and CTGF promotes migration and invasion of melanoma cells.[46] Loss of CTGF, either in melanoma or in tumor stroma, did not affect proliferation and tumor growth but diminished the ability of melanoma cells to invade and decreased spontaneous metastases of melanoma cells from the skin to the lungs.[48] Inhibition of CTGF, either genetically or with a specific anti-CTGF monoclonal antibody (FG-3019), significantly inhibited the ability of melanoma cells to grow in the skin and establish distant metastases in the lungs of SCID mice.[19] Therefore, CTGF is considered as a therapeutic target for metastatic melanoma. Regulation of *CTGF* expression is complex and largely depends on the cell type and the microenvironment.[50] In melanoma, CTGF was induced by hypoxia through HIF-1- and HIF-2-dependent mechanisms.[19,46] Our results provide initial evidence that in ^{V600E}BRAF melanoma cells, *CTGF* expression is ERK1/2-dependent, and therefore, can be downregulated by inhibitors of ^{V600E}BRAF and MEK1/2. It was demonstrated, however, that in three paired tumor biopsies *CTGF* expression was markedly upregulated after development of resistance to vemurafenib.[51] Our analysis of RNA sequencing data available at https://www.ncbi.nlm.nih.gov/geo/ revealed that changes in the *CTGF* expression after development of drug resistance are not so unambiguous (Supplementary Figure 3 and Supplementary Table 1). The development of resistance to targeted therapy (designated as progression) was accompanied by downregulated expression of *CTGF* in melanomas from 20 out of the 39 patients. Interestingly, all early during treatment samples expressed *CTGF* at lower levels than the paired drug-naive samples (Supplementary Figure 3 and Supplementary Table 1). Thus, clinical data although still limited and performed with diverse therapeutics targeting the RAF/MEK/ERK pathway, support our finding on influence of targeted therapy on expression of *CTGF*, but also *CXCL8* (Supplementary Figure 3 and Supplementary Table 1). By using parthenolide that simultaneously reduces NF-κB activity and induces ERK1/2 phosphorylation, it was possible to increase *CTGF* transcript level in melanoma cells, which further suggests that CTGF expression depends on ERK1/2 activity but not NF-κB activity. Thus, the reduced expression of CTGF was rather a consequence of the BRAF/MEK/ERK pathway inhibition than a drug off-target effect, however, further studies are necessary to elucidate the exact mechanism(s).

In summary, the present study while confirming cytostatic activity of vemurafenib and trametinib in melanoma cells also shows: (i) a drug-induced inhibition of IL-8 expression accompanied by diminished NF-κB activity; and (ii) ERK1/2-dependent reduction of CTGF expression. All these effects occurred despite the differences in the phenotype of investigated melanoma cell populations. The only exception was induction of apoptosis, which was triggered by vemurafenib and trametinib only in cell populations with the low level of active β-catenin. In the light of published reports about the contribution of IL-8 and CTGF to melanoma development, these newly uncovered effects of vemurafenib and trametinib are highly desired. In turn, the drug-induced expression of CD271, a marker of melanoma stem-like cells, is an unwanted consequence of targeted therapy shown in this study. Lack of response of melanoma stem-like cells to targeted therapy should be addressed in the development of combination treatment of melanoma patients, although a potent drug against cancer stem-like cells is not yet available.

DISCLOSURE/CONFLICT OF INTEREST
The authors declare no conflict of interest.

1. Flaherty KT, Infante JR, Daud A, *et al*. Combined BRAF and MEK inhibition in melanoma with BRAF V600 mutations. N Engl J Med 2012;367:1694–1703.
2. Merlino G, Herlyn M, Fisher DE, *et al*. The state of melanoma: challenges and opportunities. Pigment Cell Melanoma Res 2016;29: 404–416.
3. Ho AW, Tsao H.. Targeted therapies in melanoma: translational research at its finest. J Invest Dermatol 2015;135:1929–1933.
4. Su F, Viros A, Milagre C, *et al*. RAS mutations in cutaneous squamous-cell carcinomas in patients treated with BRAF inhibitors. N Engl J Med 2012;366:207–215.
5. Roesch A, Paschen A, Landsberg J, *et al*. Phenotypic tumour cell plasticity as a resistance mechanism and therapeutic target in melanoma. Eur J Cancer 2016;59:109–112.
6. Tirosh I, Izar B, Prakadan SM, *et al*. Dissecting the multicellular ecosystem of metastatic melanoma by single-cell RNA-seq. Science 2016;352:189–196.
7. Hartman ML, Talar B, Noman MZ, *et al*. Gene expression profiling identifies microphthalmia-associated transcription factor (MITF) and Dickkopf-1 (DKK1) as regulators of microenvironment-driven alterations in melanoma phenotype. PLoS One 2014;9:e95157.
8. Sztiller-Sikorska M, Hartman ML, Talar B, *et al*. Phenotypic diversity of patient-derived melanoma populations in stem cell medium. Lab Invest 2015;95:672–683.
9. Sztiller-Sikorska M, Koprowska K, Majchrzak K, *et al*. Natural compounds' activity against cancer stem-like or fast-cycling melanoma cells. PLoS One 2014;9:e90783.
10. Hartman ML, Talar B, Sztiller-Sikorska M, *et al*. Parthenolide induces MITF-M downregulation and senescence in patient-derived MITF-M (high) melanoma cell populations. Oncotarget 2016;7:9026–9040.
11. Boiko AD, Razorenova OV, van de Rijn M, *et al*. Human melanoma-initiating cells express neural crest nerve growth factor receptor CD271. Nature 2010;466:133–137.
12. Girouard SD, Murphy GF.. Melanoma stem cells: not rare, but well done. Lab Invest 2011;91:647–664.
13. Lee N, Barthel SR, Schatton T.. Melanoma stem cells and metastasis: mimicking hematopoietic cell trafficking? Lab Invest 2014;94:314–322.
14. Garraway LA, Widlund HR, Rubin MA, *et al*. Integrative genomic analyses identify MITF as a lineage survival oncogene amplified in malignant melanoma. Nature 2005;436:117–122.
15. Hartman ML, Czyz M.. Pro-survival role of MITF in melanoma. J Invest Dermatol 2015;135:352–358.
16. Wellbrock C, Arozarena I.. Microphthalmia-associated transcription factor in melanoma development and MAP-kinase pathway targeted therapy. Pigment Cell Melanoma Res 2015;28:390–406.
17. Yang K, Wang X, Zhang H, *et al*. The evolving roles of canonical WNT signaling in stem cells and tumorigenesis: implications in targeted cancer therapies. Lab Invest 2016;96:116–136.
18. Kuphal S, Lodermeyer S, Bataille F, *et al*. Expression of Dickkopf genes is strongly reduced in malignant melanoma. Oncogene 2006;25:5027–5036.
19. Finger EC, Cheng CF, Williams TR, *et al*. CTGF is a therapeutic target for metastatic melanoma. Oncogene 2014;33:1093–1100.
20. Singh S, Singh AP, Sharma B, *et al*. CXCL8 and its cognate receptors in melanoma progression and metastasis. Future Oncol 2010;6:111–116.
21. Sztiller-Sikorska M, Koprowska K, Jakubowska J, *et al*. Sphere formation and self-renewal capacity of melanoma cells is affected by the microenvironment. Melanoma Res 2012;22:215–224.
22. Koprowska K, Hartman ML, Sztiller-Sikorska M, *et al*. Parthenolide enhances dacarbazine activity against melanoma cells. Anticancer Drugs 2013;24:835–845.
23. Wozniak M, Szulawska-Mroczek A, Hartman ML, *et al*. Parthenolide complements the cell death-inducing activity of doxorubicin in melanoma cells. Anticancer Res 2013;33:3205–3212.
24. Talar B, Gajos-Michniewicz A, Talar M, *et al*. Pentoxifylline inhibits WNT signalling in β-cateninhigh patient-derived melanoma cell populations. PLoS One 2016;11:e0158275.
25. Strizzi L, Hardy KM, Kirsammer GT, *et al*. Embryonic signaling in melanoma: potential for diagnosis and therapy. Lab Invest 2011;91: 819–824.
26. Marzuka A, Huang L, Theodosakis N, *et al*. Melanoma treatments: advances and mechanisms. J Cell Physiol 2015;230:2626–2633.
27. Tap WD, Gong KW, Dering J, *et al*. Pharmacodynamic characterization of the efficacy signals due to selective BRAF inhibition with PLX4032 in malignant melanoma. Neoplasia 2010;12:637–649.
28. Haferkamp S, Borst A, Adam C, *et al*. Vemurafenib induces senescence features in melanoma cells. J Invest Dermatol 2013;133:1601–1609.
29. Sinnberg T, Makino E, Krueger MA, *et al*. A nexus consisting of beta-catenin and Stat3 attenuates braf inhibitor efficacy and mediates acquired resistance to vemurafenib. EBioMedicine 2016;8:132–149.
30. Damsky WE, Curley DP, Santhanakrishnan M, *et al*. β-catenin signaling controls metastasis in Braf-activated Pten-deficient melanomas. Cancer Cell 2011;20:741–754.
31. Chien AJ, Haydu LE, Biechele TL, *et al*. Targeted BRAF inhibition impacts survival in melanoma patients with high levels of Wnt/ β-catenin signaling. PLoS One 2014;9:e94748.
32. Zubrilov I, Sagi-Assif O, Izraely S, *et al*. Vemurafenib resistance selects for highly malignant brain and lung-metastasizing melanoma cells. Cancer Lett 2015;361:86–96.
33. Lehraiki A, Cerezo M, Rouaud F, *et al*. Increased CD271 expression by the NF-kB pathway promotes melanoma cell survival and drives acquired resistance to BRAF inhibitor vemurafenib. Cell Discov 2015;1: 15030.
34. Redmer T, Welte Y, Behrens D, *et al*. The nerve growth factor receptor CD271 is crucial to maintain tumorigenicity and stem-like properties of melanoma cells. PLoS One 2014;9:e92596.
35. Frederick DT, Piris A, Cogdill AP, *et al*. BRAF inhibition is associated with enhanced melanoma antigen expression and a more favorable tumor microenvironment in patients with metastatic melanoma. Clin Cancer Res 2013;19:1225–1231.
36. Wilson BJ, Saab KR, Ma J, *et al*. ABCB5 maintains melanoma-initiating cells through a proinflammatory cytokine signaling circuit. Cancer Res 2014;74:4196–4207.
37. Frank NY, Schatton T, Kim S, *et al*. VEGFR-1 expressed by malignant melanoma-initiating cells is required for tumor growth. Cancer Res 2011;71:1474–1485.
38. Lin CH, Wang YH, Chen YW, *et al*. Transcriptional and post-transcriptional regulation of CXCL8/IL-8 gene expression induced by connective tissue growth factor. Immunol Res 2016;64:369–384.
39. Bleau AM, Planque N, Perbal B.. CCN proteins and cancer: two to tango. Front Biosci 2005;10:998–1009.
40. Chen PP, Li WJ, Wang Y, *et al*. Expression of Cyr61, CTGF, and WISP-1 correlates with clinical features of lung cancer. PLoS One 2007;2:e534.
41. Bennewith KL, Huang X, Ham CM, *et al*. The role of tumor cell-derived connective tissue growth factor (CTGF/CCN2) in pancreatic tumor growth. Cancer Res 2009;69:775–784.
42. Dhar A, Ray A.. The CCN family proteins in carcinogenesis. Exp Oncol 2010;32:2–9.
43. Lin BR, Chang CC, Chen RJ, *et al*. Connective tissue growth factor acts as a therapeutic agent and predictor for peritoneal carcinomatosis of colorectal cancer. Clin Cancer Res 2011;17:3077–3088.
44. Chien W, O'Kelly J, Lu D, *et al*. Expression of connective tissue growth factor (CTGF/CCN2) in breast cancer cells is associated with increased migration and angiogenesis. Int J Oncol 2011;38:1741–1747.
45. Yeger H, Perbal B.. The CCN family of genes: a perspective on CCN biology and therapeutic potential. J Cell Commun Signal 2007;1: 159–164.
46. Braig S, Wallner S, Junglas B, *et al*. CTGF is overexpressed in malignant melanoma and promotes cell invasion and migration. Br J Cancer 2011;105:231–238.
47. Sha W, Leask A.. CCN2 expression and localization in melanoma cells. J Cell Commun Signal 2011;5:219–226.
48. Hutchenreuther J, Vincent KM, Carter DE, *et al*. CCN2 expressionby tumor stroma is required for melanoma metastasis. J Invest Dermatol 2015;135:2805–2813.
49. Hoek K, Rimm DL, Williams KR, *et al*. Expression profiling reveals novel pathways in the transformation of melanocytes to melanomas. Cancer Res 2004;64:5270–5282.
50. Cicha I, Goppelt-Struebe M.. Connective tissue growth factor: context-dependent functions and mechanisms of regulation. Biofactors 2009;35:200–208.
51. Sun C, Wang L, Huang S, *et al*. Reversible and adaptive resistance to BRAF(V600E) inhibition in melanoma. Nature 2014;508:118–122.